

DD

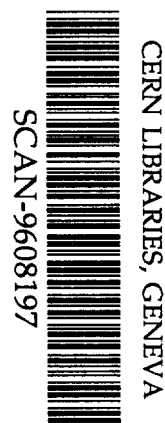


LAPP-EXP-96.09
JUNE 1996

THE NOMAD EXPERIMENT :

A Status Report

Jean-Marie Gaillard
LAPP - F74941 Annecy-Le-Vieux



SW9636

Presented on behalf of the Nomad Collaboration
2nd International Symposium on
Sources and Detection of Dark Matter in the Universe
February 14-16,1996 - Santa-Monica, Californie

THE NOMAD EXPERIMENT : A Status Report*

Jean-Marc Gaillard, LAPP
F-74941 Annecy-le-Vieux

1. INTRODUCTION

The main goal of the NOMAD experiment [1,2] - Neutrino Oscillation

MAGnetic Detector - is to search for $\nu_\mu \rightarrow \nu_\tau$

oscillations through the appearance of ν_τ neutrinos in the CERN SPS wide-band beam. In absence of oscillations the beam

composition is $\nu_\mu : \bar{\nu}_\mu : \nu_e : \bar{\nu}_e : \nu_\tau$
 $1 : 6 \times 10^{-2} : 7 \times 10^{-3} : 2 \times 10^{-3} : 10^{-7}$,

with a negligible ν_τ fraction compared to the sensitivity of the experiment. The presence of neutrino oscillations is detected by searching for the charged current interactions :

$$\begin{aligned} \nu_\tau + N &\rightarrow \tau^- + X ; \\ \tau^- &\rightarrow \text{decay products} + \nu_\tau \end{aligned} \quad (1)$$

(at our beam energies the kinematical suppression of the cross-section is $\sigma_\tau^{\text{CC}} / \sigma_\mu^{\text{CC}} \approx 0.56$). For two family mixing, the probability of observing an oscillation at a distance L is given by :

$$\begin{aligned} P(\nu_\mu \rightarrow \nu_\tau) &= \sin^2 2\theta \sin^2 \pi \frac{L}{\lambda}; \\ \lambda(\text{km}) &\approx \frac{2.48 E_\nu(\text{GeV})}{\Delta m^2(\text{eV}^2)} \end{aligned} \quad (2)$$

where θ is the mixing angle, L is the distance between the neutrino production and observation, λ is the oscillation length determined by the neutrino energy E_ν and the eigenstates squared mass difference $\Delta m^2 \equiv m_2^2 - m_3^2$. NOMAD is located at a distance $L = 900$ m from the target and is exposed to neutrinos with an average energy of 27 GeV and hence is sensitive to the region $\Delta m^2 > 1 \text{ eV}^2$. The expectations for NOMAD [2] and CHORUS [3], in the case of a negative result after two years of running, are shown in fig. 1 together with earlier experimental limits [4-7].

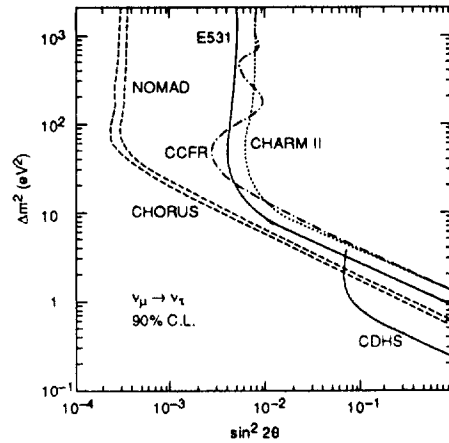


Figure 1.

* Talk presented on behalf of the NOMAD Collaboration.

2. THE NOMAD DETECTOR

The NOMAD detector (fig. 2) was designed to identify and to measure electrons, muons, photons and hadrons produced in neutrino interactions. The capability to track individual particles in neutrino interactions makes the detector similar to an "electronic bubble chamber". As an example, a reconstructed ν_μ current charge interaction candidate taken during the 1995 run is shown in Figure 3.

A detailed description of the detector has been given elsewhere [2]. With the exception of a forward veto plane and rear muon chambers, the NOMAD subdetectors are housed inside the recycled UA1 detector magnet which provides a dipole horizontal magnetic field of 0.4 T perpendicular to the beam axis over a volume of $3.6 \times 3.5 \times 7.0 \text{ m}^3$.

The subdetectors are :

- the **drift chambers**, located in the magnetic field, which play the role of target with a fiducial mass of about 2700 kg, a low average density $\approx 100 \text{ kg/m}^3$ and a $1 X_0$ thickness. Charged particles are reconstructed with little degradation from multiple scattering given the low Z of the chamber material : $\Delta p/p \approx 4\%$ for $p < 20 \text{ GeV/c}$.

- the **transition radiation detector**, (TRD) to tag electrons on a large area of $3 \times 3 \text{ m}^2$, composed of nine identical planes, giving a rejection factor for pions over electrons

$\approx 10^3$ for particles of incident energy above 2 GeV.

- the **electromagnetic calorimeter** [8] (ECAL), an array of 35×25 lead glass counters $19 X_0$ deep, with $\Delta E_{em}/E_{em} \approx 4\%/\sqrt{E_{em}} \oplus 1\%$, preceded by the **preshower** (PS), a $1.6 X_0$ lead converter and two orthogonal arrays of 288 proportional tubes.

- the **hadronic calorimeter**, (HCAL) made of 23 iron slabs with 20 instrumented gaps, 6.2λ sampled and $\Delta E_H/E_H \approx 100\%/\sqrt{E_H}$.

- the **muon chambers** consisting of 10 drift chambers previously used in the UA1 experiment arranged in pairs for track segment reconstruction (active area $3.75 \times 5.55 \text{ m}^2/\text{chamber}$).

- the **forward calorimeter**, (FCAL), mass 17 tons and area $\approx 1.9 \times 1.5 \text{ m}^2$, placed in front of the active target which provides neutrino flux measurements with $\Delta E/E \approx 100\%/\sqrt{E}$.

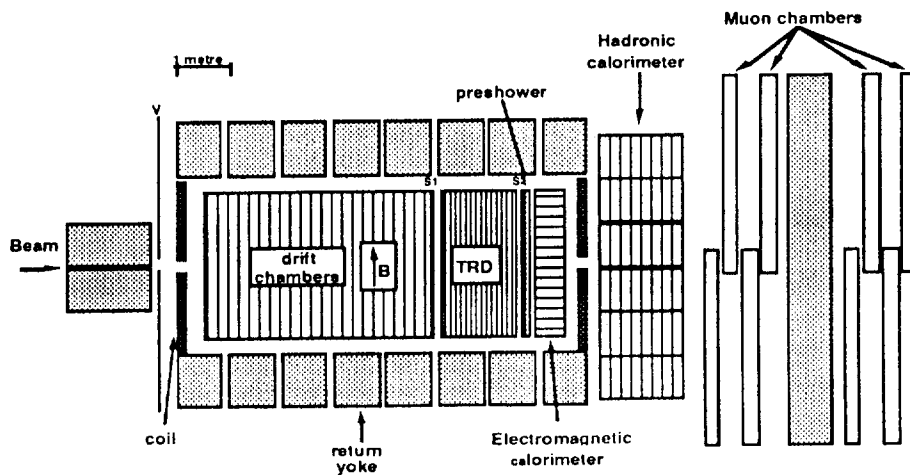


Figure 2. Top view (x-z view) of the NOMAD detector.

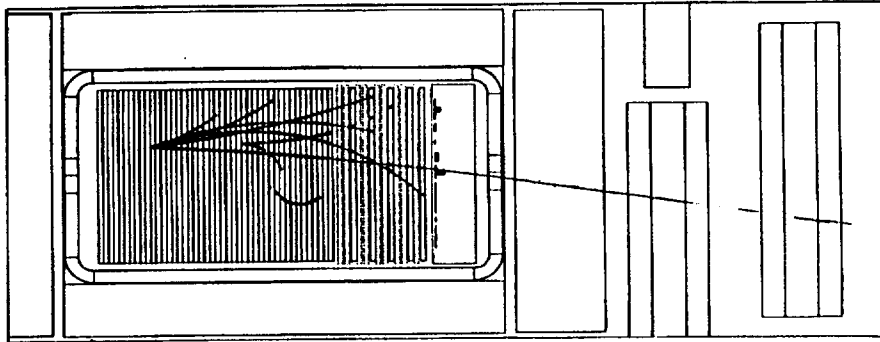


Figure 3. ν_μ charged current event (side view).

3. DETECTOR PERFORMANCE

The 1995 run can be divided into three major periods. The first (Period A : 2.8×10^{18} protons on target (p. o. t.)) when only 4/11 of the target was instrumented because of delays introduced in chamber construction. A second phase started in the beginning of July when 8/11 of the target was put into operation (Period B : 3.0×10^{18} p.o.t.). Finally, in the third period the drift chambers were fully installed (Period C : 3.1×10^{18} p.o.t.). The 1995 run went very smoothly with all subdetectors functioning well.

Using the data of periods B and C, studies of the performance of the detectors were made. Detailed information about tracking accuracy, muon and charged hadron measurements as well as neutrino energy reconstruction can be found elsewhere [9]. From the inclusive muon signed momentum spectrum a 2.7% μ^+/μ^- ratio was measured which yields a flux ratio $\phi(\bar{\nu})/\phi(\nu) \approx 6\%$ in agreement with the expectation. The distribution of the reconstructed neutrino energy (10 - 200 GeV) agrees with the Monte Carlo expectation where the energy resolution is $\approx 18\%$.

Photons and neutral hadrons are measured in the calorimeters. In the reconstruction, tracks are extrapolated to the

calorimeter front face and calorimetric "clusters" are assigned to them. The unassigned cells are regrouped into neutral clusters. The invariant mass of pairs of neutral clusters from neutrino interactions is shown in Figure 4. with a peak at the π^0 mass ($\sigma \approx 11 \text{ MeV}/c^2$). The invariant mass distribution of single isolated neutral clusters and e^+e^- pairs reconstructed in the drift chamber target - i.e. two tracks of opposite charge originating from a secondary vertex with an e^+e^- reconstructed mass $< 100 \text{ MeV}/c^2$ - shows a π^0 peak with a comparable resolution (fig. 5).

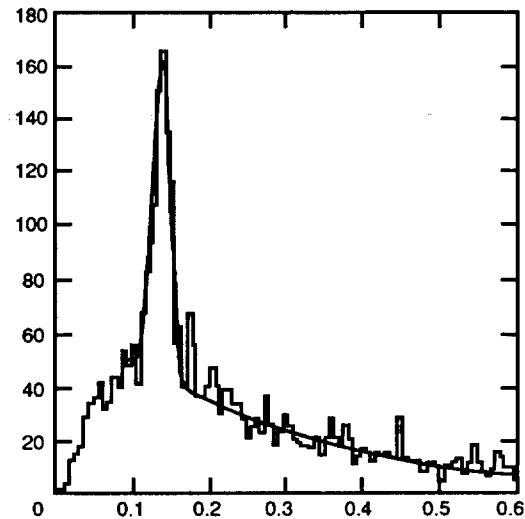


Figure 4. $\gamma\gamma$ invariant mass (GeV/c^2).

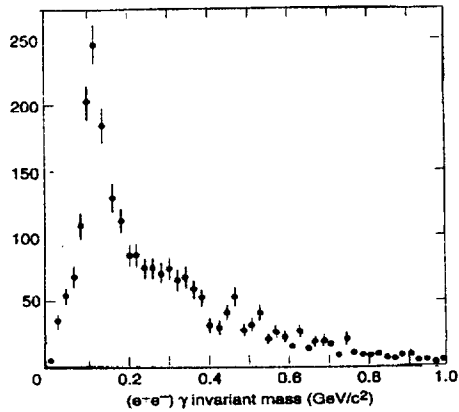


Figure 5. $(e^+ e^-) \gamma$ invariant mass.

4. ELECTRON IDENTIFICATION

The search for $\tau \rightarrow e$ decay signatures as evidence for $\nu_\mu \rightarrow \nu_\tau$ oscillations in the Nomad experiment requires a powerful electron identification system. For momenta larger than 1 GeV/c, a rejection factor of 10^4 against charged hadrons and an electron efficiency of $\sim 80\%$ are achieved by combining requirements on :

- the pulse heights in the 9 TRD modules.
- the PS and the ECAL measurements: shape of the shower profile, size of the preshower signal, comparison between the amount of energy E deposited in the calorimeter and the track momentum P at the front face of the calorimeter.

Typically an electron gives a large transition radiation signal in the TRD and deposits all of its energy in ECAL. Most of the charged hadrons reaching the ECAL deposit instead only a fraction of their energy (average pion deposit 1.4 GeV for $p = 5$ GeV/c). The results of applying the electron identification criteria, separately and in combination, to all the tracks in

neutrino charged current interactions are shown in the $(E-P)/(E+P)$ distributions of Figure 6.

High energy electrons are produced in charged current interactions of ν_e 's present in the beam at a level of $\sim 0.6\%$ with respect to ν_μ 's. The electron identification procedure was applied to events without an identified muon in the data. Additional cuts remove conversion background. The momentum distribution of the selected "electrons" is compared to Monte Carlo expectations in Figure 7. The observed agreement is a check of the quality of the electron identification.

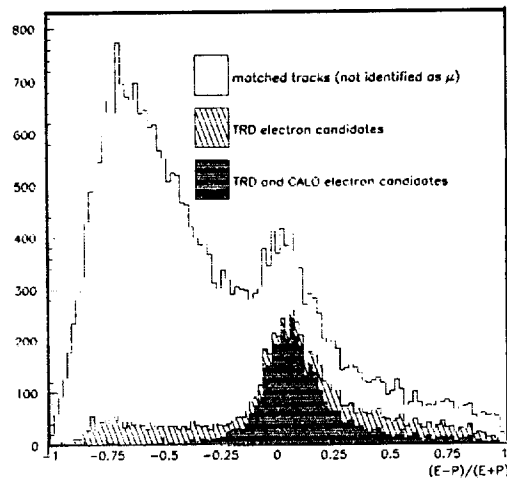


Figure 6. $(E-P)/(E+P)$ distributions.

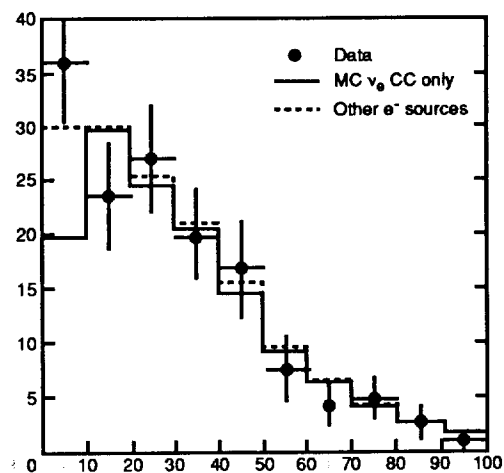


Figure 7. Electron momentum (GeV/c).

Table 1.
Decay modes of the tau lepton used in the search for oscillations.

Channel	B. R.	ϵ	B. R. $\times \epsilon$	N_{τ}^*
$\tau^- \rightarrow e^- \bar{\nu}_e \nu_{\tau}$	18.0%	13.5%	2.4%	39
$\tau^- \rightarrow \mu^- \bar{\nu}_{\mu} \nu_{\tau}$	17.6%	3.9%	0.7%	11
$\tau^- \rightarrow \pi^- \nu_{\tau}$	11.7%	1.4%	0.2%	3
$\tau^- \rightarrow \rho^- (\pi^- \pi^0) \nu_{\tau}$	25.2%	2.0%	0.5%	7
$\tau^- \rightarrow \pi^* \pi^- \pi^- + n \pi^0 \nu_{\tau}$	14.4%	7.7%	1.1%	18

B. R. is the decay branching ratio, ϵ is the estimated efficiency after all selection cuts [1]. N_{τ}^* is the number of expected events for oscillation with mixing parameter $\sin^2 2\theta_{\mu\tau} = 5 \times 10^{-3}$ for large Δm^2 and $1.1 \times 10^6 \nu_{\mu} \text{CC}$.

5. NEUTRINO TAU SEARCH

The experiment looks for neutrino oscillations by searching for ν_{τ} appearance. The decay channels used to search for τ^- produced in ν_{τ} charged current interactions are listed in Table 1. The selection cuts which suppress backgrounds yield efficiencies for the signal ranging from 13.5% for the electron channel down to a few percent for the hadronic decay modes. The estimated sensitivity for oscillation searches is based on $1.1 \times 10^6 \text{CC } \nu_{\mu}$ events, $375 \times 10^3 \text{NC } \nu_{\mu}$ events and $13 \times 10^3 \text{CC } \nu_e$ events. The N_{τ}^* column represents the number of expected events after selection cuts if oscillations occur at the level of $\sin^2 2\theta_{\mu\tau} = 5 \times 10^{-3}$ for large Δm^2 - i.e. at the present limit. In total, one would expect to see 78 signal events over a background of 7.0 events. The expected backgrounds are 4.6(2.2) events for the electron (muon) channel and small (< 0.2) for the hadronic channels. The search methods, which vary according to the decay channel studied, have been described in more detail elsewhere [1, 2].

6. CONCLUSIONS

The NOMAD detector performed well during the 1995 run. The instrumented target was completed during August 1995 and a significant amount of data was acquired. The 1996 run has started and a similar run has been approved for 1997 with the aim to collect more than a million neutrino charged current interactions. For the data taken in 1995, the analysis is progressing. Electrons, muons, hadrons and neutrals are well identified and measured in the various subdetectors. The search for neutrino oscillations is in progress.

REFERENCES.

1. NOMAD Collab., P. Astier et al., CERN-SPSLC/91-21 (1991), CERN-SPSLC/91-48 (1991), SPSLC/P261 Add. 1 (1991), CERN-SPSLC/93-31.
2. NOMAD Collab., J. Altegoer et al., NOMAD MEMO 95-027. Contribution to the EPS HEP '95 International Conference on High Energy Physics, August 1995, Brussels, Belgium.

3. K. Kodama, these proceedings; CHORUS Collab., N. Armenise et al., CERN-SPSC/90-42 (1990); CHORUS Collab., M. de Jong et al., CERN-PPE/93-131.
4. N. Ushida et al., Phys. Rev. Lett. 57 (1986) 2897.
5. M. Gruwe et al., CHARM-II Collab., Phys. Lett. B309 (1993) 463.
6. K. S. McFarland, CCFR Collab. et al., Phys. Rev. Lett. 75 (1995) 3993.
7. F. Dydak et al., CDHS Collab., Phys. Lett. B134 1984 (281).
8. D. Autiero et al., "The electromagnetic calorimeter of the NOMAD experiment", submitted to Nuclear Instr. & Methods in Phys. Research.
9. A. Rubbia, to be published in Proceedings of the 7th International Workshop on Neutrino Telescopes, Venice, Italy, 1996.

